Turkish Journal of Earth Sciences (Turkish J. Earth Sci.), Vol. 18, 2009, pp. 529–547. Copyright ©TÜBİTAK
doi:10.3906/yer-0811-8 First published online 30 April 2009

# Contemporaneous Late Cretaceous Calc-alkaline and Alkaline Magmatism in Central Anatolia, Turkey: Oxygen Isotope Constraints on Petrogenesis

NURDANE İLBEYLİ[1], JULIAN A. PEARCE[2],
IAN G. MEIGHAN[3] & ANTHONY E. FALLICK[4]

[1] Mustafa Kemal University, İskenderun Campus, Faculty of Engineering, TR–31200 Hatay, Turkey
(E-mail: nurilbeyli@yahoo.com)

[2] Cardiff University, Department of Earth Sciences, PO Box 914, Cardiff, CF10 3YE, UK

[3] Dublin University, Department of Geology, Dublin 2, Ireland

[4] SUERC, Scottish Enterprise Technology Park, Rankine Avenue, East Kilbridge, G75 0QF, UK

*Received 21 November 2008; revised typescript received 03 March 2009; accepted 04 March 2009*

**Abstract:** A wide variety of rock types were produced by the latest Cretaceous magmatism in the Central Anatolian Crystalline Complex. These rocks can be divided into three distinct units: (i) calc-alkaline, (ii) subalkaline/transitional, and (iii) alkaline. The calc-alkaline rocks are mainly metaluminous (I-type) ranging from monzodiorite to granite. The subalkaline/transitional rocks are also metaluminous (I-type) ranging from monzonite to granite. The alkaline rocks are mainly peralkaline (A-type), ranging from feldspathoid-bearing monzosyenite to granite. Whole-rock oxygen isotope data from the complex have a considerable range of $\delta^{18}O$ values between 6.5‰ and 14.8‰. Initial $^{87}Sr/^{86}Sr$ versus $^{143}Nd/^{144}Nd$ ratios, and both ratios versus $\delta^{18}O$ values diagrams show that the intrusive rocks are derived from a subduction-modified mantle and also have experienced fractional crystallisation coupled with crustal assimilation. Delamination of a thermal boundary layer, and/or slab breakoff is the likely mechanisms for the initiation of the diverse magmatism in the complex.

**Key Words:** I-type granite, A-type granite, oxygen isotope, Kaman-Kırşehir region, central Anatolia, Turkey

## Orta Anadolu'da Eş zamanlı Geç Kretase Kalkalken ve Alkalen Magmatizma (Türkiye): Petrojenezde Oksijen İzotop Kısıtlamaları

**Özet:** Orta Anadolu Kristalen Kompleksi içerisinde yeralan farklı türdeki kayaç tipleri geç Kretase magmatizması ile üretilmiştir. Bu kayaçlar üç farklı birime ayırt edilmiştir: (i) kalkalkalen, (ii) yarıalkalen/geçişli, ve (iii) alkalen. Kalkalkalen kayaçlar genelde metalüminüs (I-tip) olup, bileşimleri monzodiyoritden granite kadar değişir. Yarıalkalen/geçişli kayaçlar da metalüminüs (I-tip) olup, bileşimleri monzonitden granite kadar değişir. Alkalen kayaçlar genelde peralkalen (A-tip) olup, bileşimleri feldispatoyidli monzosiyenitden granite kadar değişir. Kompleksdeki tüm kaya oksijen izotop verileri 6.5‰ ve 14.8‰ arasında önemli oranlardaki $\delta^{18}O$ değerlerine sahiptir. İlksel $^{87}Sr/^{86}Sr$-$^{143}Nd/^{144}Nd$ oranları, ve her iki oran-$\delta^{18}O$ diyagramları göstermektedir ki intrüzif kayaçlar dalma-batma ile değişikliğe uğramış mantodan türemiş ve ayrıca fraksiyonal kristalleşme ve kabuksal kirlenme geçirmiştir. Kompleks de farklı magmatizmaların başlangıcı için uygun mekanizmalar ya termal sınır tabakasının delaminasyonu ya da dalmakta olan levhanın (kırılıp?) yok edilmesidir (slab breakoff).

**Anahtar Sözcükler:** I-tipi granit, A-tipi granit, oksijen izotop, Kaman-Kırşehir bölgesi, Orta Anadolu, Türkiye

## Introduction

The Alpine-Mediterranean region is one of the most complex geodynamic settings on Earth. In this region, subduction, collision and extension have occurred, associated with the formation of a wide variety of igneous rocks during pre-Tertiary, Tertiary

(subject of this study) and Quaternary times (Şengör & Yılmaz 1981). The large compositional diversity is caused by (1) different source compositions, (2) variable melting conditions, (3) complex chemical and physical interactions between mafic and felsic magmas, and (4) crustal contamination. Interpretation of results from petrogenetic studies in this region not only provides constraints on the geodynamic processes, but also reveals changes in magma source regions. One of the principal features of collision-related magmatism is its subduction-related geochemical characteristics, despite subduction processes having been terminated as a result of continental collision. The subduction-related signatures of these magmatic rocks are mainly attributed to metasomatism by slab-derived fluids of the mantle lithosphere prior to collision (e.g., Pearce *et al.* 1990; Platt & England 1993; Turner *et al.* 1996). Thus, the geochemical characteristics of collision-related magmatism allow the evaluation of subduction-related metasomatism of their mantle source.

Oxygen isotopes provide a tracer of subducted materials that were once part of the continental crust. The oxygen isotope composition is particularly useful because one can use simply binary mixing equations to perform calculations.

Intrusive rocks are abundant in the central Anatolian region and reveal a wide range of fabrics, mineral assemblages and compositions. The $\delta^{18}O$ values of the central Anatolian intrusive rocks are scarce (e.g., Tatar & Boztuğ 2005; Önal *et al.* 2005; Boztuğ & Arehart 2007; Boztuğ *et al.* 2007a). In this paper, we present new oxygen isotope data from the key plutons in central Anatolia to establish the compositional differences of the magma sources and the processes responsible for the generation of this wide variety of magmas. The combination of oxygen isotope data with existing whole-rock, Sr, Nd geochemistry and geochronologic data also have been used in the paper to obtain a petrogenetic model for the diverse magmatism in the complex.

## Geological Background

The Central Anatolian Crystalline Complex is made up of several metamorphic massifs (Akdağmadeni, Kırşehir, Niğde), numerous granitic to syenitic plutons and dismembered ophiolites, and Tertiary volcanic and sedimentary rocks that unconformably overlie the crystalline rocks (Göncüoğlu *et al.* 1991) (Figure 1). The massifs constitute the nucleus of the complex and consist of gneisses, schists, amphibolites and marbles displaying different *P-T-t* trajectories (e.g., Whitney *et al.* 2001). Studies concerning the ages of the main metamorphic events suggest a Late Cretaceous age (Late Campanian–Early Maastrichtian) (Whitney *et al.* 2003; Whitney & Hamilton 2004).

Ophiolitic rocks occur in thrust sheets over the massifs and represent dismembered remnants of the Neo-Tethyan oceanic lithosphere. Ophiolitic assemblages in the eastern part of the complex (Figure 1) are composed mainly of serpentinised peridotites with a significant listwaenite occurrence along their sheared contacts with the metamorphic massifs (e.g., Boztuğ *et al.* 1997), whereas those exposed in the west consist essentially of gabbro, diabase and individual basaltic dykes (e.g., Yalınız & Göncüoğlu 1998). Most ophiolitic rocks are Late Cretaceous (excluding metamorphosed equivalents) and of supra-subduction type, derived from the closure of the northern branch of the Neo-Tethyan Ocean (e.g. Yalınız *et al.* 1996).

Although the crystallisation ages for the central Anatolian intrusive rocks are still debated, radiogenic age determinations mainly indicate Late Cretaceous–Palaeocene ages (e.g., Whitney *et al.* 2003; İlbeyli *et al.* 2004; Köksal *et al.* 2004; Boztuğ & Jonckheere 2007; Boztuğ *et al.* 2007b; Boztuğ & Harlavan 2008; Boztuğ *et al.* 2009a, b).

## Petrology and Petrochemistry

Summaries of the field, petrographic, mineralogical and geochemical characteristics of the intrusive rocks from the Central Anatolian Crystalline Complex are presented in Table 1. The magmatic activity in the complex began during the Late Cretaceous and created both calc-alkaline and alkaline products (e.g., İlbeyli 2004, 2005; İlbeyli *et al.* 2004; Boztuğ & Arehart 2007) (Figure 2) (Table 1).

Samples from the Behrekdağ, Cefalıkdağ, and Çelebi intrusions have been chosen as

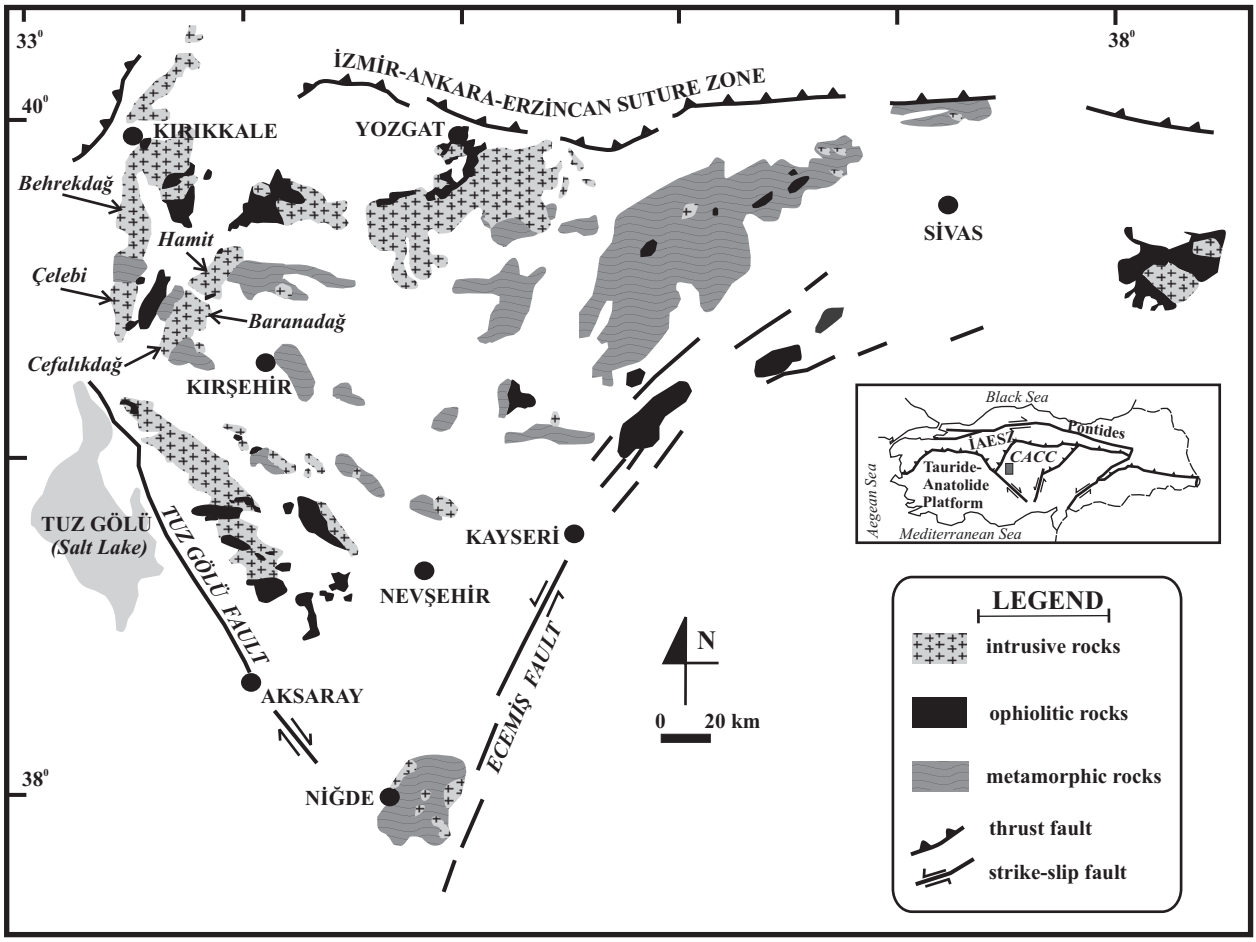


**Figure 1.** Geological setting of the Central Anatolian Crystalline Complex (modified from Bingöl 1989). Abbreviations: CACC– Central Anatolian Crystalline Complex, İAESZ– İzmir-Ankara-Erzincan Suture Zone.

representatives of the calc-alkaline rocks, samples from the Baranadağ intrusion are representative of the subalkaline/transitional rocks and samples from the Hamit intrusion are representative of the alkaline rocks (Figure 1). Details of the geological setting, mineralogical and geochemical characteristics and geochronological data of these intrusive rocks can be found in İlbeyli (2004, 2005) and İlbeyli *et al.* (2004), and are summarised in Table 1.

## Analytical Methods

Ten samples were selected for oxygen isotope analyses. Inclusions such as mafic enclaves and xenoliths were removed from the samples. Oxygen isotope ratios were measured at the Scottish Universities Environment and Research Centre, United Kingdom. Oxygen was extracted by reacting 1–2 mg of sample with purified chlorine trifluoride in a laser fluorination system, based on Sharp (1990). The oxygen was converted to $CO_2$ by reaction on a hot graphite rod, and its isotopic composition was analysed on a VG PRISM III mass spectrometer. All oxygen ratios are in the standard per mil notation relative to VSMOW (Vienna Standard Mean Ocean Water). Multiple analyses of NBS 28 reference sample quartz give a mean value of 9.6‰. An accepted value for this reference sample is 9.84‰ (Coplen *et al.* 1983). Precision estimated through regular analysis of internal quartz standard (SES at 10.2‰) was 0.2‰ (1σ).

**Table 1.** Classification of the central Anatolian intrusive rocks on the basis of their field, petrography, mineralogy and major element geochemistry.

| **Pluton** | **Behrekdağ, Cefalıkdağ, Çelebi** | **Baranadağ** | **Hamit** |
|---|---|---|---|
| **Age** | Late Cretaceous to Palaeocene | Late Cretaceous to Palaeocene | Late Cretaceous to Palaeocene |
| **Mineral composition** | Ksp+Pl (albite to andesine) +Qtz+Amp (edenite, magnesio-hornblende)+Bt±Cpx (salite) | Ksp+Pl (oligoclase to andesine) +Qtz+Amp (edenite, magnesio-hastingsite)+Bt±Cpx (salite) | Ksp+Pl (albite to labradorite) ±Qtz±Amp (edenite, hastingsite) ±Bt±Cpx (salite)±Ne±Grt (melanite) |
| **Grain size** | fine- through medium- to porphyritic with feldspar (up to 15 cm across) | coarse- to porphyritic with feldspar (up to 5 cm across) | fine- to porphyritic with alkali feldspar (up to 3.5 cm across) |
| **Texture** | allotriomorphic to porphyritic | allotriomorphic to porphyritic | hypidiomorphic to porphyritic |
| **Accessory phases** | titanite, opaques, apatite, zircon, allanite | titanite, opaques, apatite, zircon, allanite | titanite, opaques, apatite, zircon, fluorite |
| **Alteration** | sericite, chlorite, calcite, epidote | sericite, chlorite, calcite | cancrinite, gieseckite, garnet, sericite, chlorite, epidote |
| **Rock type (see Figure 2)** | mzdi, qmzdi, mz, qmz, grd, gr | mz, qmz | feldspathoid-bearing (nepheline, pseudoleucite) sy *(the least silicic);* feldspathoid-free (mz, qmz, sy, kspsy, qsy) (*the most silicic*) |
| **$K_2O$ composition** | high-K to shoshonite | high-K to shoshonite | high-K to shoshonite |
| **Shand's index** | metaluminous / peraluminous | metaluminous | mostly peralkaline |

**Table 1.** Continued.

| **Pluton** | **Behrekdağ, Cefalıkdağ, Çelebi** | **Baranadağ** | **Hamit** |
|---|---|---|---|
| **Alkali-lime index** | calc-alkalic | alkali-calcic | alkalic |
| **Rare earth element patterns (Chondrite-normalised, Boynton 1984)** | all LREE-enriched with small to moderate negative Eu anomalies | all LREE-enriched with small to moderate negative Eu anomalies | all LREE-enriched with small to moderate negative Eu anomalies |
| **Multi-element patterns (ORG-normalised, Pearce *et al.* 1984)** | enrichment in the LILE (K, Rb, Ba, Th) and the LREE (Ce) relative to the HFSE (Ta, Nb, Hf, Zr, Sm, Y, Yb). | enrichment in the LILE and the LREE relative to the HFSE | enrichment in the LILE and the LREE relative to the HFSE |
| **Tectonic discrimination diagrams (Pearce *et al.* 1984)** | fall into the VAG (volcanic arc granite) and syn-COLG (syn-collisional granite) fields | plot between the VAG and syn-COLG and WPG (within plate granite) fields. | fall in the WPG field |
| | ***CALC-ALKALINE*** | ***SUBALKALINE / TRANSITIONAL*** | ***ALKALINE*** |
| **Granite type** | **I- / S-** *(the least silicic-I )* *(the most silicics)* | **I- / A-** | **A-** *(the most silicic-S )* |
| **References** | İlbeyli *et al.* (2004) İlbeyli (2005) | İlbeyli *et al.* (2004) İlbeyli (2005) | İlbeyli *et al.* (2004) İlbeyli (2004, 2005) |

Abbreviations: Ksp– alkali feldspar, Pl– plagioclase, Qtz– quartz, Amp– amphibole, Bt– biotite, Cpx– clinopyroxene, Ne– nepheline, Grt– garnet; mzdi– monzodiorite, qmzdi– quartz monzodiorite, mz– monzonite, qmz– quartz monzonite, grd– granodiorite, gr– granite, sy– syenite, kspsy– alkali feldspar syenite, qsy– quartz syenite.

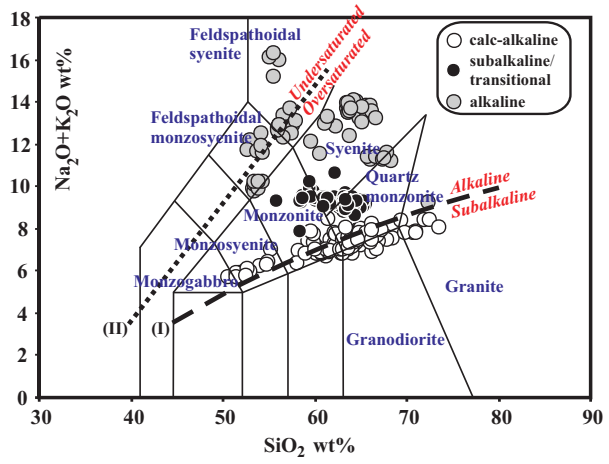


**Figure 2.** Classification of the central Anatolian plutonic rocks (Middlemost 1994) using the total alkali-silica diagram. *Line (I)* separates the alkaline and subalkaline field of Miyashiro (1978) and *line (II)* separates the alkaline oversaturated and undersaturated series (Giret & Lameyre 1980).

The full data set is given in Table 2. Major, trace element and radiogenic isotope data of these rock samples are also presented in Table 3.

## Oxygen Isotope Geochemistry

Whole-rock oxygen isotope data from the Central Anatolian Crystalline Complex have a large range of $\delta^{18}O$ values between 6.5‰ and 14.8‰ (Figure 3) (Table 2). The calc-alkaline rocks have $\delta^{18}O$ values ranging from 8.4‰ to 11.1‰ (Figure 3). The subalkaline/transitional rock has only one analysis, which has a $\delta^{18}O$ value of 8.3‰ (Figure 3).

The lowest $\delta^{18}O$ (6.5‰) value is represented by the feldspathoid-bearing rock (sample N33) and the highest value (12.1‰) belongs to the feldspathoid-free rock (sample N290) of the alkaline samples (Figure 3) (Table 2). A metasedimentary rock (sample C-2) from central Anatolia has a $\delta^{18}O$ value 14.8‰. Typical oxygen isotopic compositions for MORB (mid ocean ridge basalt) are between 5.2‰ and 6.4‰ (Eiler *et al.* 2000). I-type granitoids have $\delta^{18}O$ values of 6 to 10‰, whereas S-type granitoids display higher $\delta^{18}O$ values of 10 to 15‰ (Harris *et al.* 1997) and A-type granitoids have $\delta^{18}O$ values of 6 to 8‰ (Whalen *et al.* 1996).

Oxygen isotope ratios were analysed on mineral separates (e.g., zircon) in preference to whole-rock samples because the latter is susceptible to changes in $\delta^{18}O$ values resulted by later hydrothermal alteration (e.g., Valley *et al.* 1994; King *et al.* 1998; Monani & Valley 2001). Although alteration at surface temperatures causes an increase in $\delta^{18}O$ values, meteoric alteration in continental systems lowers $\delta^{18}O$ values (e.g., Gregory & Criss 1986; Larson & Taylor 1986; Criss *et al.* 1987; Taylor 1997; Jung *et al.* 2007).

**Table 2.** O isotope data of the intrusive rocks from the Central Anatolian Crystalline Complex. $\delta^{18}O$ values reported in per mil relative to VSMOW.

| Pluton / Area | Characteristics | Rock unit | Sample no | $\delta^{18}O$, per mil |
|---|---|---|---|---|
| **Behrekdağ** | *calc-alkaline* | quartz monzonite | N2 | 10.3 |
| **Cefalıkdağ** | *calc-alkaline* | quartz monzodiorite | N78 | 9.4 |
| | | quartz monzonite | N20 | 9.9 |
| | | granite | N395 | 11.1 |
| **Çelebi** | *calc-alkaline* | quartz monzonite | N75 | 8.4 |
| **Baranadağ** | *subalkaline/transitional* | monzonite | N26 | 8.3 |
| **Hamit** | *alkaline* | nepheline syenite | N33 | 6.5 |
| | | nepheline syenite | N285 | 7.6 |
| | | quartz syenite | N290 | 12.1 |
| **Central Anatolia (Kırşehir)** | | metasediment | C-2 | 14.8 |

**Table 3.** XRF-major element (wt%), trace element (ppm) and ICP-MS-rare earth elements (ppm) analyses of the representative samples from the central Anatolian intrusive rocks (İlbeyli 1999, 2005; İlbeyli *et al.* 2004).

| **Pluton / Area** | Behrekdağ | Cefalıkdağ | | | Çelebi | Baranadağ | Hamit | | Kırşehir | | |
|---|---|---|---|---|---|---|---|---|---|---|---|
| **Sample no** | **N2** | **N78** | **N20** | **N395** | **N75** | **N26** | **N33** | **N285** | **N290** | **N490** | **C-2** |
| **Rock unit** | *qmz* | *qmzd* | *qmz* | *gr* | *qmz* | *mz* | *nesy* | *nesy* | *qsy* | *metagreywacke* | *metapelite* |
| **$SiO_2$** | 60.11 | 53.86 | 61.82 | 71.53 | 65.07 | 58.44 | 53.32 | 56.09 | 66.78 | 74.96 | 77.52 |
| **$TiO_2$** | 0.61 | 0.85 | 0.61 | 0.20 | 0.39 | 0.59 | 0.72 | 0.51 | 0.28 | 0.17 | 0.39 |
| **$Al_2O_3$** | 16.49 | 17.70 | 16.36 | 14.37 | 15.81 | 17.62 | 18.09 | 20.42 | 17.32 | 12.52 | 11.21 |
| **$Fe_2O_3$** | 6.04 | 8.22 | 5.77 | 1.98 | 4.34 | 5.42 | 6.49 | 4.44 | 1.79 | 1.61 | 3.87 |
| **MnO** | 0.12 | 0.15 | 0.12 | 0.05 | 0.09 | 0.13 | 0.15 | 0.12 | 0.05 | 0.02 | 0.06 |
| **MgO** | 2.42 | 3.74 | 2.52 | 0.61 | 1.46 | 1.85 | 2.97 | 1.08 | 0.29 | 0.71 | 2.10 |
| **CaO** | 6.38 | 8.22 | 5.14 | 1.97 | 4.33 | 5.95 | 7.01 | 3.59 | 1.59 | 1.57 | 0.45 |
| **$Na_2O$** | 2.94 | 2.99 | 2.99 | 2.82 | 3.13 | 3.73 | 3.37 | 4.93 | 4.29 | 2.14 | 0.74 |
| **$K_2O$** | 3.89 | 3.23 | 4.19 | 5.37 | 4.54 | 5.52 | 6.71 | 7.99 | 7.30 | 5.58 | 2.84 |
| **$P_2O_5$** | 0.18 | 0.27 | 0.19 | 0.06 | 0.14 | 0.24 | 0.42 | 0.25 | 0.04 | 0.03 | 0.07 |
| **L.O.I** | 0.37 | 0.78 | 0.51 | 0.79 | 0.54 | 0.58 | 1.05 | 0.77 | 0.64 | 1.12 | 2.57 |
| **TOTAL** | 99.18 | 99.24 | 99.71 | 98.96 | 99.30 | 99.48 | 99.25 | 99.42 | 99.72 | 99.32 | 99.25 |
| **Sc** | 15 | 23 | 13 | 4 | 9 | 12 | 8 | 3 | 1.8 | 4.7 | 16 |
| **Cr** | 28 | 35 | 22 | | 7 | 5 | 40 | 21 | 3.0 | 4.6 | 323 |
| **V** | 91 | 144 | 93 | 12 | 63 | 102 | 123 | 52 | 24.5 | 18.7 | 45 |
| **Ni** | 12 | 16 | 9 | 2 | 9 | 14 | 15 | 5 | 1.4 | 0.9 | 7 |
| **Co** | 13 | 24 | 14 | 2 | 10 | 12 | 13 | 7 | 10.5 | 2.0 | 85 |
| **Cu** | 12 | 24 | 2 | | 1 | | 34 | 25 | 2.7 | 19.9 | 13 |
| **Zn** | 78 | 95 | 81 | 38 | 55 | 91 | 108 | 96 | 26.7 | 11.9 | 56 |
| **Ga** | 16 | 23 | 20 | 15 | 19 | 22 | 26 | 20 | 19.7 | 11.9 | 15 |
| **Rb** | 132 | 87 | 142 | 171 | 185 | 193 | 226 | 256 | 368.8 | 261.6 | 135 |
| **Sr** | 548 | 903 | 510 | 331 | 456 | 911 | 1294 | 1391 | 240.4 | 84.5 | 50 |
| **Y** | 26 | 26 | 30 | 1.9 | 28 | 36 | 40 | 33 | 40.4 | 20.7 | 28 |
| **Zr** | 177 | 187 | 176 | 127 | 145 | 277 | 369 | 375 | 316.1 | 124.2 | 165 |
| **Nb** | 14 | 18 | 16 | 10 | 14 | 26 | 28 | 35 | 35.2 | 13.5 | 11 |
| **Ba** | 1042 | 1435 | 961 | 686 | 788 | 933 | 1248 | 1345 | 308.8 | 662.1 | 413 |
| **La** | 56.60 | 43.64 | 59.18 | 25.27 | 49.86 | 89.24 | 112.68 | 103.84 | 117.64 | 25.51 | 28.67 |
| **Ce** | 95.69 | 82.10 | 103.27 | 45.19 | 91.06 | 157.48 | 208.86 | 160.73 | 177.54 | 47.66 | 56.06 |

**Table 3**. Continued.

| **Pluton / Area** | Behrekdağ | Cefalıkdağ | | | Çelebi | Baranadağ | Hamit | | Kırşehir | | |
|---|---|---|---|---|---|---|---|---|---|---|---|
| **Sample no** | **N2** | **N78** | **N20** | **N395** | **N75** | **N26** | **N33** | **N285** | **N290** | **N490** | **C-2** |
| **Rock unit** | *qmz* | *qmzd* | *qmz* | *gr* | *qmz* | *mz* | *nesy* | *nesy* | *qsy* | *metagreywacke* | *metapelite* |
| **Pr** | 10.59 | 10.04 | 12.05 | 5.00 | 10.53 | 17.75 | 23.03 | 19.71 | 15.80 | 5.60 | 6.90 |
| **Nd** | 35.59 | 38.40 | 42.19 | 16.50 | 36.35 | 60.12 | 76.77 | 66.56 | 45.68 | 19.98 | 25.98 |
| **Sm** | 5.84 | 7.20 | 7.14 | 2.50 | 6.04 | 9.90 | 13.57 | 10.00 | 6.11 | 3.97 | 5.25 |
| **Eu** | 1.37 | 1.83 | 1.40 | 0.88 | 1.17 | 2.01 | 2.89 | 2.27 | 1.00 | 0.41 | 0.68 |
| **Gd** | 4.59 | 5.96 | 5.61 | 1.57 | 4.36 | 6.39 | 9.58 | 6.72 | 3.92 | 3.46 | 4.37 |
| **Tb** | 0.73 | 0.85 | 0.88 | 0.22 | 0.69 | 1.01 | 1.00 | 0.86 | 0.62 | 0.60 | 0.77 |
| **Dy** | 3.98 | 4.67 | 4.86 | 1.18 | 3.78 | 5.20 | 5.16 | 4.12 | 3.21 | 3.81 | 4.56 |
| **Ho** | 0.79 | 0.89 | 0.94 | 0.23 | 0.78 | 0.97 | 0.83 | 0.74 | 0.63 | 0.82 | 0.94 |
| **Er** | 2.14 | 2.42 | 2.68 | 0.60 | 2.10 | 2.60 | 2.14 | 1.94 | 1.89 | 2.19 | 2.34 |
| **Tm** | 0.36 | 0.34 | 0.44 | 0.11 | 0.36 | 0.43 | 0.32 | 0.31 | 0.34 | 0.39 | 0.42 |
| **Yb** | 2.18 | 2.14 | 2.74 | 0.68 | 2.31 | 2.64 | 2.25 | 1.92 | 2.27 | 2.41 | 2.62 |
| **Lu** | 0.36 | 0.34 | 0.45 | 0.12 | 0.39 | 0.42 | 0.32 | 0.29 | 0.37 | 0.37 | 0.39 |
| **Hf** | 5.16 | 5.43 | 5.82 | 3.21 | 4.38 | 6.91 | 7.32 | 7.39 | 7.30 | 3.51 | 4.55 |
| **Ta** | 0.96 | 0.85 | 1.32 | 0.28 | 1.49 | 1.74 | 2.13 | 2.62 | 1.94 | 0.65 | 1.00 |
| **Pb** | 41.74 | 34.08 | 43.19 | 37.72 | 47.55 | 38.69 | 51.51 | 72.67 | 67.57 | 34.23 | 13.04 |
| **Th** | 22.34 | 11.17 | 23.23 | 14.88 | 36.89 | 30.19 | 50.91 | 62.00 | 106.99 | 21.40 | 11.06 |
| **U** | 4.48 | 3.08 | 5.07 | 2.90 | 5.69 | 5.29 | 13.72 | 18.15 | 13.24 | 3.06 | 3.33 |
| **$^{87}Sr/^{86}Sr$ (±1σ)** | 0.71004±11 | 0.70972±09 | 0.71002±08 | 0.71087±19 | 0.71028±35 | 0.70873±11 | 0.70875±12 | 0.70876±11 | 0.71275±09 | | |
| **(meas)** | | | | | | | | | | | |
| **$^{87}Sr/^{86}Sr_i$** | 0.70923 | 0.70943 | 0.70924 | 0.70964 | 0.70900 | 0.70804 | 0.70826 | 0.70822 | 0.70838 | | |
| **εSr (70 Ma)** | 68.5 71 | 68.4 | 74 | 64.7 | 51.6 | 54.6 | 54 | 56.3 | | | |
| **$^{143}Nd/^{144}Nd$ (±1σ)** | 0.512263±4 | 0.512256±5 | 0.512295±5 | 0.512300±5 | 0.512298±5 | 0.512324±5 | 0.512349±5 | 0.512348±5 | 0.512307±5 | | |
| **(meas)** | | | | | | | | | | | |
| **$^{143}Nd/^{144}Nd_i$** | 0.51220 | 0.51221 | 0.51225 | 0.51226 | 0.51225 | 0.51227 | 0.51230 | 0.51230 | 0.51223 | | |
| **εNd (70 Ma)** | -6.3 | -6.7 | -5.9 | -5.7 | -5.5 | -5.2 | -4.8 | -4.8 | -5.5 | | |

Abbreviations: qmz– quartz monzonite, qmzd– quartz monzodiorite, gr– granite, mz– monzonite, nesy– nepheline syenite, qsy– quartz syenite.

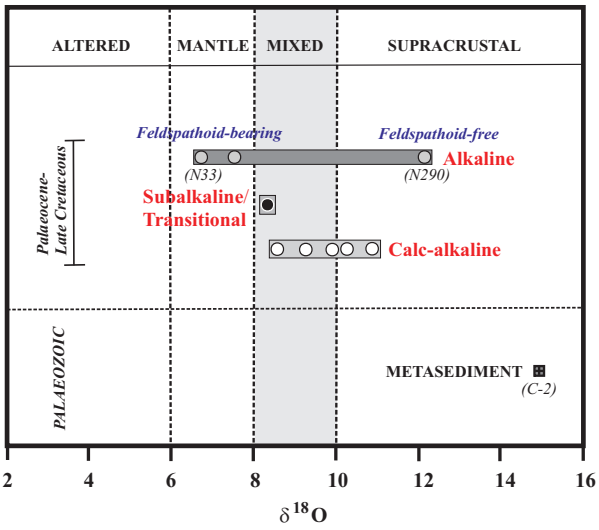


**Figure 3.** $\delta^{18}O$ values of the intrusive rocks and crust (metasediment) from central Anatolia. Dividing lines between altered, mantle, mixed and supracrustal rocks are taken from Whalen *et al.* (1996).

The values obtained for the central Anatolian intrusive rocks may represent primary values or may result from hydrothermal alteration that changes $\delta^{18}O$ values. Field evidence and petrographic observations of the central Anatolian intrusive rocks suggest that hydrous alteration was limited. Since the representative intrusive rocks have fresh and unaltered appearances in the field, most whole-rock loss-on-ignition (LOI) values are less than 1 wt%, and only one sample (N33) has a value of 1.05 wt% LOI (Figure 4) (Table 4). This could indicate limited amounts of volatiles in the samples.

Hydrous alteration under oxidising conditions results in enrichment of the whole-rock $Fe^{3+}/Fe^{2+}$ ratio (Jung *et al.* 2007). The $Fe^{3+}/Fe^{2+}$ ratios also correlate positively with the LOI values during these conditions (Jung *et al.* 2007). The $Fe^{3+}/Fe^{2+}$ ratio vs LOI, $Fe^{3+}/Fe^{2+}$ ratio vs $\delta^{18}O$ and $\delta^{18}O$ vs LOI may provide an indication of the extent to which such alteration influenced the stable isotope chemistry of the rocks analysed (Figure 4). There is a lack of positive correlation between $Fe^{3+}/Fe^{2+}$ and LOI for the intrusive rocks (Figure 4a), indicating that they are not altered. The $Fe^{3+}/Fe^{2+}$ ratios vs $\delta^{18}O$ values (Figure 4b) show that there is also no correlation between $Fe^{3+}/Fe^{2+}$ and $\delta^{18}O$. The $\delta^{18}O$ values display negative trends with LOI for the calc-alkaline and alkaline rocks (Figure 4c). Although some meteoric alteration is probable in the alkaline rocks, the correlations (Figure 4) could suggest that the alteration was not important to any considerable extent. The positive correlation of $\delta^{18}O$ values with initial $^{143}Nd/^{144}Nd$ ratios (largely insensitive with respect to hydrous alteration; Jung *et al.* 2007) for the intrusive rocks reveals that they are not altered (see below Figure 7: inset figures). Therefore we can assume that the $\delta^{18}O$ values of the intrusive rocks could be primary.

## Discussion

The central Anatolian intrusive rocks are enriched in LILE relative to HFSE (İlbeyli *et al.* 2004). In addition, they are radiogenic in terms of Sr, and unradiogenic in terms of Nd isotope ratios (İlbeyli *et al.* 2004). These features could be related to combined crustal assimilation and fractional crystallisation (AFC) (e.g., Hildreth & Moorbath 1988) or to mantle source enrichment by recycling of crustal material (e.g., Gill 1981; Sun & McDonough 1989).

Initial $^{87}Sr/^{86}Sr$ ratios of the plutonic rocks are plotted against initial $^{143}Nd/^{144}Nd$ ratios (Figure 5) to reveal AFC or source enrichment processes in the origin of central Anatolian intrusive rocks. All rock types plot in the high initial $^{87}Sr/^{86}Sr$ and low initial $^{143}Nd/^{144}Nd$ quadrant in the range characteristic of continental crustal sources or mantle sources with large continental crustal components (Figure 5a).

Calculation of AFC curves are model-dependent, since they require presumptions about the fractionating mineral assemblages and mineral-melt partition coefficients, the concentrations of the chosen trace elements in the starting melt and the contaminant(s) as well as the ratio of assimilation to fractional crystallisation (Jung *et al.* 2004).

Estimation of the compositions of possible source component(s) and also crustal contaminant(s) is a very difficult problem for the central Anatolian intrusive rocks, as there are no rock samples that can be taken as representative of a parental magma(s) (see Discussion section; İlbeyli 2005). Therefore, the chosen values for the parental magmas are close to

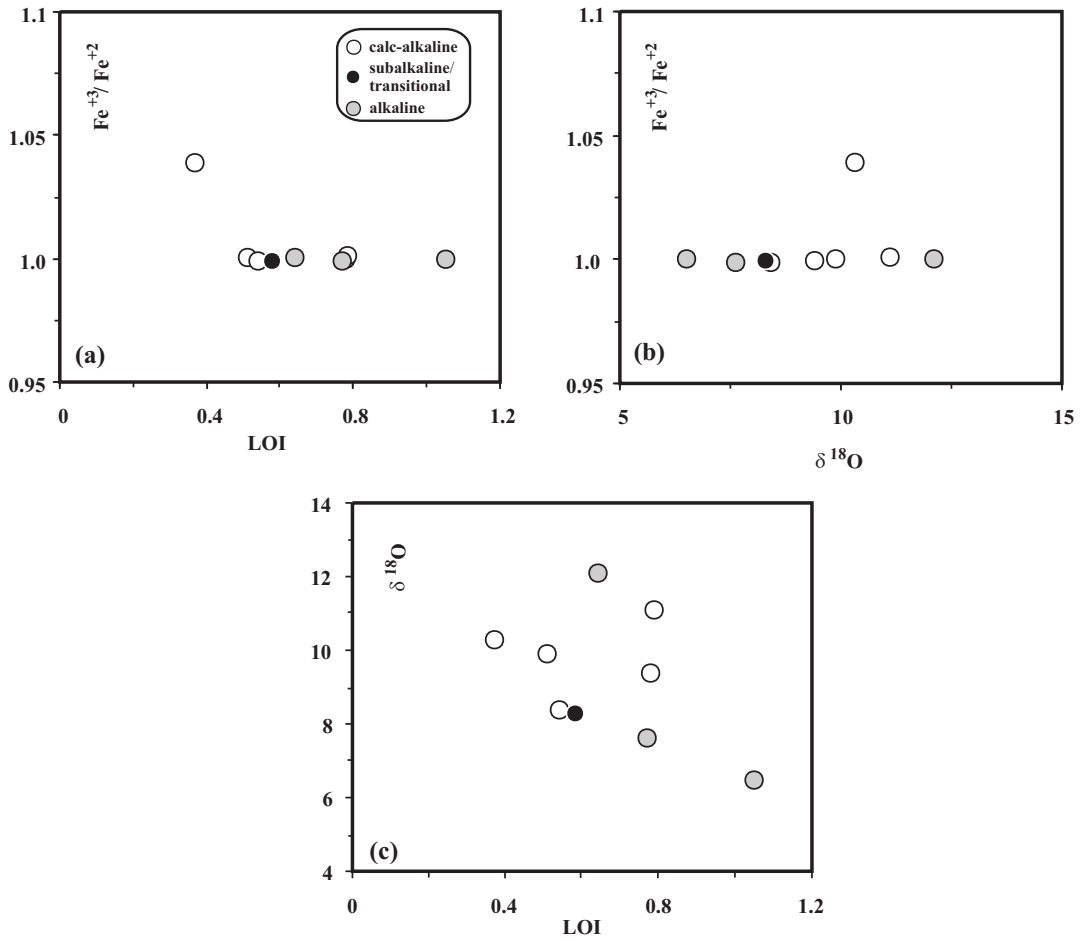


**Figure 4.** **(a)** $Fe^{3+}/Fe^{2+}$ versus LOI; **(b)** $Fe^{3+}/Fe^{2+}$ versus $\delta^{18}O$; and **(c)** $\delta^{18}O$ versus LOI diagrams for the central Anatolian intrusive rocks.

**Table 4.** Loss-on-ignition (LOI), $Fe_2O_3$ and FeO values and $Fe^{3+}/Fe^{2+}$ ratios of the intrusive rocks from the Central Anatolian Crystalline Complex.

| Pluton | Sample no | LOI (wt%) | $Fe_2O_{3\ (total)}$ (wt%) | FeO (wt%) | $Fe^{3+}/Fe^{2+}$ |
|---|---|---|---|---|---|
| **Behrekdağ** | N2 | 0.37 | 6.04 | 5.23 | 1.04 |
| **Cefalıkdağ** | N78 | 0.78 | 8.22 | 7.40 | 0.99 |
| | N20 | 0.51 | 5.77 | 5.19 | 1.00 |
| | N395 | 0.79 | 1.98 | 1.78 | 1.00 |
| **Çelebi** | N75 | 0.54 | 4.34 | 3.91 | 0.99 |
| **Baranadağ** | N26 | 0.58 | 5.42 | 4.88 | 1.00 |
| **Hamit** | N33 | 1.05 | 6.49 | 5.84 | 1.00 |
| | N285 | 0.77 | 4.44 | 4.00 | 1.00 |
| | N290 | 0.64 | 1.79 | 1.61 | 0.99 |

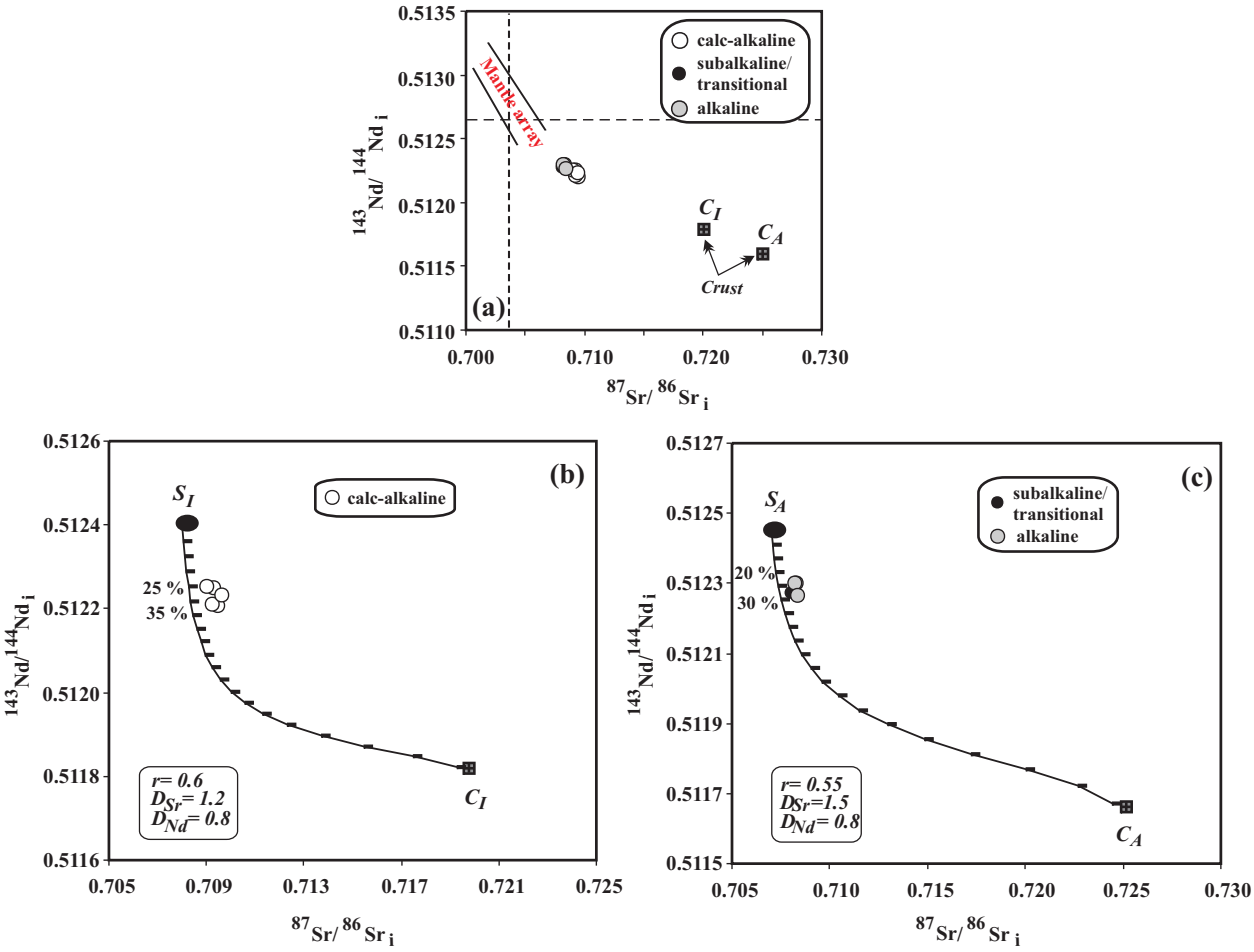


**Figure 5.** **(a)** $^{143}Nd/^{144}Nd_i$ versus $^{87}Sr/^{86}Sr_i$ diagram for the central Anatolian plutonic rocks and hypothetical basement samples. The mantle array is after DePaolo (1988); **(b)** $^{143}Nd/^{144}Nd_i$ versus $^{87}Sr/^{86}Sr_i$ plot showing AFC model for the calc-alkaline intrusive rocks; and **(c)** $^{143}Nd/^{144}Nd_i$ versus $^{87}Sr/^{86}Sr_i$ plot displaying AFC model for the subalkaline/transitional and alkaline intrusive rocks. Tick marks on each curve represent 5% crystallisation intervals (F). In this model, crystallisation ends after F reaches 0.05. Tick marks on the AFC curves represent the ratio of the final mass of magma to the initial mass of magma. Abbreviations: D– the bulk partition coefficient, F– the fraction of melt remaining, r– the ratio of the rate of assimilation to the rate of fractional crystallisation, $S_I$– source for the calc-alkaline rocks, $C_I$– crust for the calc-alkaline rocks, $S_A$– source for the subalkaline/transitional and alkaline rocks, $C_A$– crust for the subalkaline/transitional and alkaline rocks. Assumed mantle and crustal end-member compositions are given in Table 5.

those of the least acidic samples for the calc-alkaline (source I- $S_I$) and alkaline intrusive rocks (source A- $S_A$) (Table 5). Two metamorphic samples (C-2 and N490) from the Central Anatolian Crystalline Complex are used as the crustal components [crust I- $C_I$ (sample no. C-2) for the calc-alkaline samples and crust A- $C_A$ (sample no. N490) for the alkaline samples] (Figure 5, Table 5). Unfortunately, there is also insufficient Sr-Nd isotope data to define crustal end-member compositions of the complex, so possible Sr and Nd isotope compositions for C-2 and N490 are assumed (Table 5). O isotope composition is available only for C-2 (Table 2).

The AFC modelling has been conducted using the AFC equations of DePaolo (1981), the bulk partition coefficient (*D*) and the ratio of the rate of assimilation to the rate of fractional crystallisation

**Table 5.** Table showing possible parental magmas and contaminants for the central Anatolian intrusive rocks used in the petrogenetic modelling.

| | Source I ($S_I$) for the calc-alkaline rocks | Crust I ($C_I$) for the calc-alkaline rocks (sample no: C-2) | Source A ($S_A$) for the subalkaline/transitional & alkaline rocks | Crust A ($C_A$) for the subalkaline/transitional & alkaline rocks (sample no: N490) |
|---|---|---|---|---|
| $^{87}Sr/^{86}Sr_i$ | 0.7080 | 0.7200 | 0.7070 | 0.7250 |
| Sr ppm | 1000 | 50 | 1400 | 85 |
| $^{143}Nd/^{144}Nd_i$ | 0.51240 | 0.51180 | 0.51245 | 0.51160 |
| Nd ppm | 30 | 26 | 25 | 19 |
| $\delta^{18}O$ per mil | 7 | 14.8 | 5.7 | 18 |

(*r*) presented in Figure 5. All models use $D_{Sr}$ of 1.2 (for the calc-alkaline rocks) – 1.5 (for the alkaline rocks) and $D_{Nd}$ of 0.8 (for both rock types), values broadly consistent with the observed geochemical behaviour of Sr and Nd in these rocks. The modelled AFC mixing curves pass close to the plutonic rocks (Figure 5b, c). Between ~25% and ~35% upper crustal contaminant is required in the AFC modelling for the calc-alkaline rocks, whereas between ~22% and ~30% upper crustal contaminant is required in the AFC modelling for the alkaline rocks (Figure 5b, c). Such rates make assimilation acceptable because at upper crustal levels higher rates would not be possible (DePaolo 1981).

In terms of determining source(s) of contamination, oxygen isotopes also provide a potentially powerful tool because many components that can be present in the crust have differing $\delta^{18}O$ values (e.g., James 1981; Bacon *et al.* 1989; Feeley & Sharp 1995; Macpherson *et al.* 1998). The upper portion of ocean crust is shifted in $\delta^{18}O/\delta^{16}O$ because of low-temperature hydrothermal alteration and also the presence of high $\delta^{18}O$ sediments, and thus metasomatising fluids are high in $\delta^{18}O$ (Eiler *et al.* 1998; Eiler 2001). $\delta^{18}O$ values can also be shifted by assimilation or remelting of altered igneous rocks (Valley *et al.* 2005).

The $\delta^{18}O$ values of the central Anatolian plutonic rocks are plotted against $SiO_2$ (Figure 6). The intrusive rocks align along two different trends starting from two different hypothetical parental magma compositions (i.e. source $S_I$ and source $S_A$) and, crossing from each other, heading toward two separate crustal compositions (i.e. crust $C_I$ and crust $C_A$) (Figure 6). Two contrasting groups in the central Anatolian plutonic rocks can be also displayed in initial $^{87}Sr/^{86}Sr$ and $^{143}Nd/^{144}Nd$ ratios vs $SiO_2$ diagrams (see figure 8 in İlbeyli *et al.* 2004).

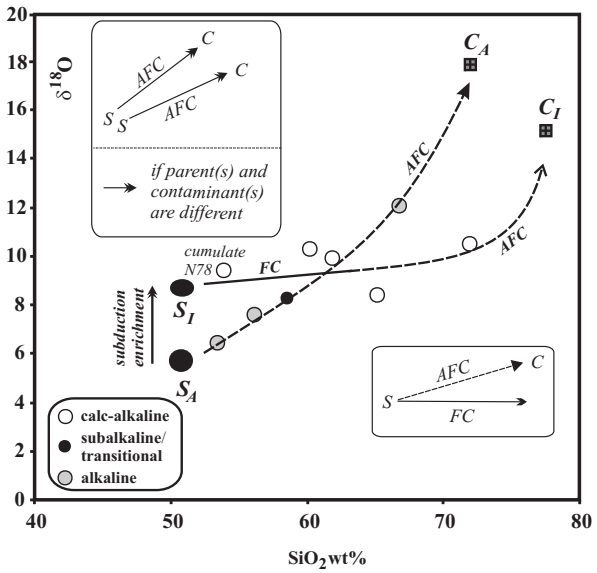


**Figure 6.** $\delta^{18}O$ values versus silica plot for the central Anatolian intrusive rocks. Abbreviations: S– source, C– crust, $S_I$– source for the calc-alkaline rocks, $C_I$- crust for the calc-alkaline rocks, $S_A$– source for the subalkaline/transitional and alkaline rocks, $C_A$– crust for the subalkaline/transitional and alkaline rocks, FC– fractional crystallisation, AFC– fractional crystallisation coupled with crustal assimilation.

The calc-alkaline rock samples are characterised by slightly higher $\delta^{18}O$ values than the alkaline rock samples (Figure 6). The contaminants have also higher $\delta^{18}O$ values (14.8–18‰) (Table 5) than the calc-alkaline and alkaline samples. Fractional crystallisation (FC) has little effect (≤ 1‰) on $\delta^{18}O$ values (Sheppard & Harris 1985), therefore oxygen isotopes are a powerful indicator of source composition and/or degree of crustal contamination. The trend for the calc-alkaline rocks indicates that the rocks have undergone mainly FC and only AFC in the latest stages. On the other hand, the $\delta^{18}O$ values of the alkaline rock samples (including the subalkaline/transitional sample) show a well-defined positive correlation with silica (Figure 6). This indicates that the evolution of the alkaline samples is governed by AFC processes and probably also some alteration processes. The higher $\delta^{18}O$ values of the calc-alkaline rocks suggest a mantle source which is more enriched in subduction components than the source of alkaline rocks (Figure 6).

The distinction between source contamination and crustal assimilation can be identified using O-Sr isotopic modelling (e.g., James 1981; Taylor 1986; Ellam & Harmon 1990). Oxygen isotope enrichment is a sensitive indicator of crustal contamination, whereas Sr isotopes can be either sensitive or insensitive to contamination (e.g., Davidson *et al.* 1990; Ellam & Harmon 1990; Mason *et al.* 1996).

The $\delta^{18}O$ values are plotted against initial $^{87}Sr/^{86}Sr$ ratios (Figure 7) to better define the process(es) causing the formation of the two trends in Figure 6 for the central Anatolian plutonic rocks. Initial $^{143}Nd/^{144}Nd$ vs $\delta^{18}O$ values are also plotted in Figure 7 as inset figures. Initial $^{87}Sr/^{86}Sr$ ratios increase with increasing $\delta^{18}O$ values, whereas initial $^{143}Nd/^{144}Nd$ ratios decrease with $\delta^{18}O$ values. We also plot theoretical trends that reflect AFC mixing models (Figure 7). The crustal material underlying the alkaline rocks is much more radiogenic in terms of Sr, and unradiogenic in terms of Nd than the one that underlies the calc-alkaline rocks (Figure 7). The calc-alkaline and alkaline samples (including one subalkaline/transitional) plot around or close to the modelled AFC trends. Between ~25% and ~55% upper crustal contaminant is required in the AFC modelling for the calc-alkaline rocks, whereas between ~15% and ~65% upper crustal contaminant is required in the AFC modelling for the alkaline rocks (Figure 7). The most silicic calc-alkaline (N395) and alkaline (N290) samples have higher assimilation (~55% for Sr; ~50% for Nd; the former) (~60% for Sr; ~65% for Nd; the latter) than the other calc-alkaline and alkaline samples.

The main variations shown by isotope data (Sr, Nd, O) (Figures 5–7) for the central Anatolian plutonic rocks can be also seen in plots of Th/Y vs Nb/Y and Nb/Zr vs Nb (Figure 8). The former plot (Figure 8a) shows that all intrusive rocks form trends that run parallel to the mantle array but are displaced towards higher Nb/Y ratios, indicating either derivation from an enriched mantle source to which subduction component had been added, or AFC, or both (İlbeyli *et al.* 2004). The Th/Y and Nb/Y ratios increase from the calc-alkaline through the subalkaline/transitional and alkaline plutonic rocks (Figure 8a). The high Nb/Y ratio of the alkaline rocks can be explained by derivation from more enrichment in a within-plate component than that of the calc-alkaline plutonic rocks. The central Anatolian plutonic rocks do not form a trend from the mantle array to the crust (Figure 8a), so AFC is not likely to have been the only process for the generation of the plutonic rocks.

Ratios of HFSE (e.g., Nb, Zr) can give useful information about magma source composition (e.g., Davidson 1996; Singer *et al.* 1996). Nb and Zr are mainly mantle-derived and strongly fractionated during melting or magma-mixing (e.g., Thirlwall *et al.* 1994; Davidson 1996). The Nb/Zr ratios are not affected by FC and crustal contamination (e.g., Seghedi *et al.* 2004). Different Nb/Zr ratios are interpreted in terms of variations in source composition and/or changes in degree of partial melting of the mantle (e.g., Thirlwall *et al.* 1994; Singer *et al.* 1996). In Figure 8b, the Nb/Zr ratios and Y increase from the calc-alkaline through the subalkaline/transitional to the alkaline plutonic rocks. The calc-alkaline rocks are closer to a MORB-like source comparable to that of the subalkaline/transitional and alkaline rocks. However, the alkaline rocks are closer to an OIB-like source (Figure 8b). Figure 8 shows that the alkaline rocks are more enriched in a within-plate component than the calc-alkaline plutonic rocks (Figure 8b).

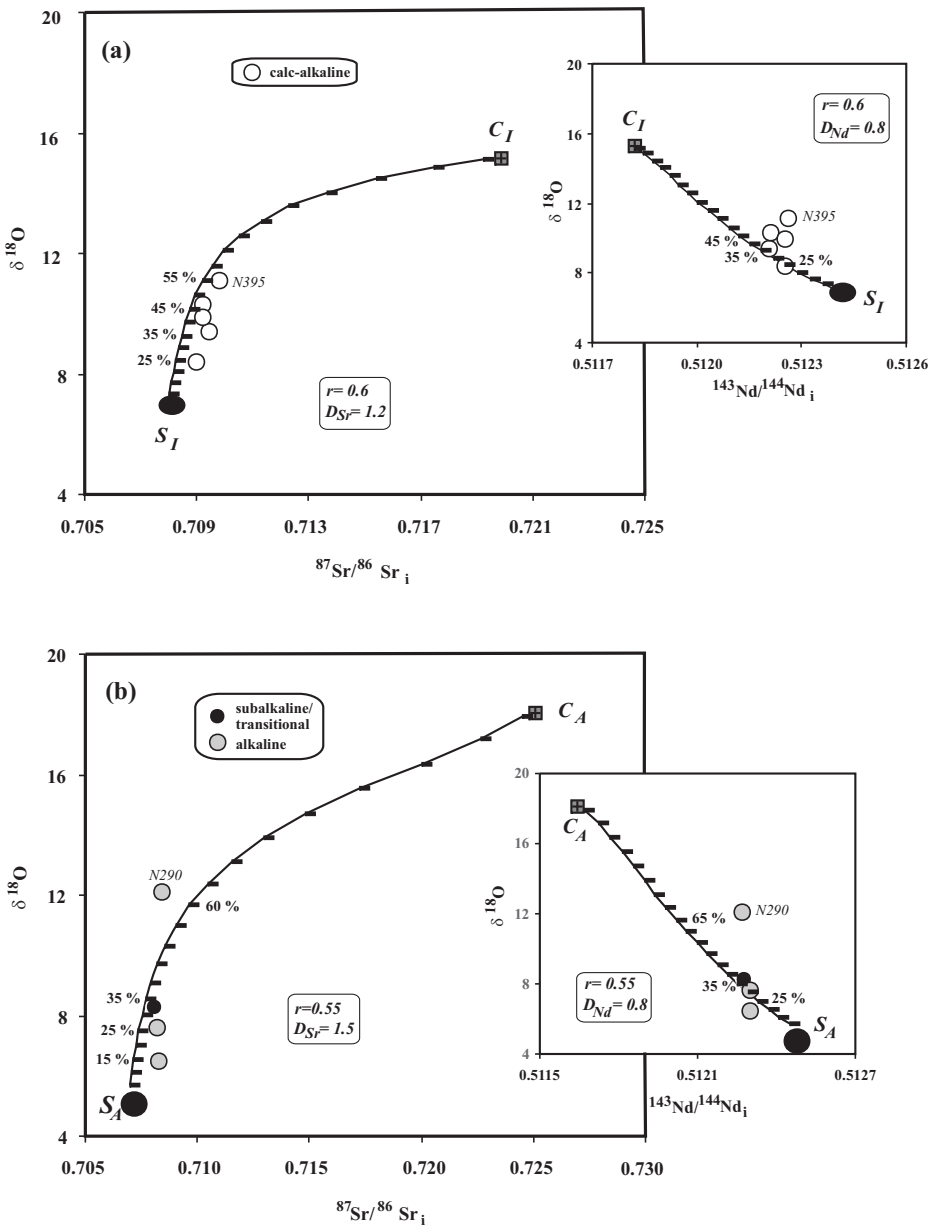


**Figure 7.** **(a)** $\delta^{18}O$ values versus $^{87}Sr/^{86}Sr_i$ diagram showing the results of AFC for the calc-alkaline intrusive rocks (inset figure: $\delta^{18}O$ vs $^{143}Nd/^{144}Nd_i$); **(b)** $\delta^{18}O$ values versus $^{87}Sr/^{86}Sr_i$ diagram displaying the results of AFC for the subalkaline/transitional and alkaline rocks (inset figure: $\delta^{18}O$ vs $^{143}Nd/^{144}Nd_i$). Tick marks on each curve represent 5% crystallisation intervals. In this model, crystallisation ends after F reaches 0.05. Tick marks on the AFC curves represent the ratio of the final mass of magma to the initial mass of magma. Abbreviations: D– the bulk partition coefficient, F– the fraction of melt remaining, r– the ratio of the rate of assimilation to the rate of fractional crystallisation, $S_I$– source for the calc-alkaline rocks, $C_I$– crust for the calc-alkaline rocks, $S_A$– source for the subalkaline/transitional and alkaline rocks, $C_A$– crust for the subalkaline/transitional and alkaline rocks.

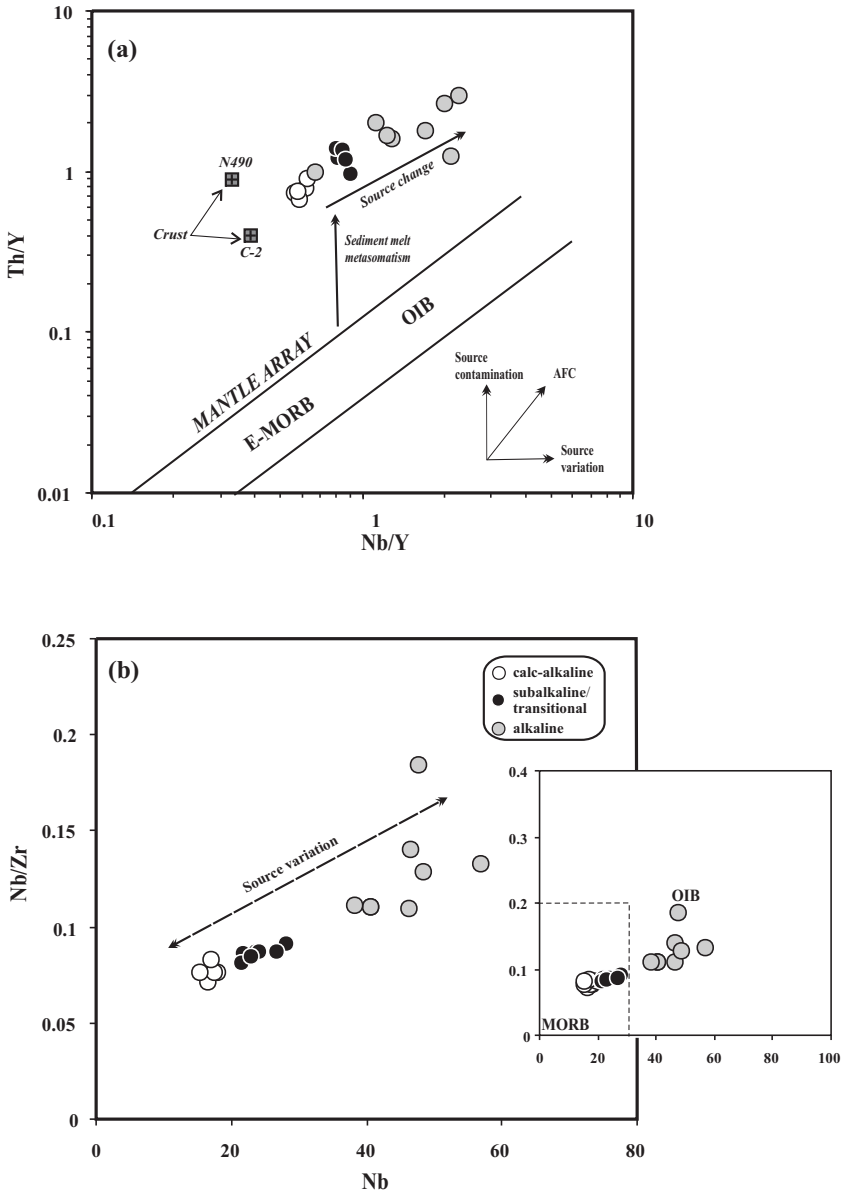


**Figure 8.** **(a)** Th/Y versus Nb/Y diagram for basic and intermediate intrusive rocks (samples <63% $SiO_2$ are plotted) (after Seghedi *et al.* 2004). **(b)** Nb/Zr versus Nb diagram for basic and intermediate intrusive rocks (after Seghedi *et al.* 2004). MORB and OIB values after Sun & McDonough (1989).

Based on the Sr-Nd-O data, it seems possible that the central Anatolian magmas were derived from a source composed of two distinct mantle and crustal components. The variations (Figures 5–8) shown by the calc-alkaline intrusive rocks could suggest that they are derived from a mantle source containing subduction components, and later experienced assimilation and fractional crystallisation processes. In contrast, the subalkaline/transitional and alkaline intrusive rocks could be derived from a more-enriched mantle source compared to the calc-alkaline intrusive rocks. These assumptions are in

general agreement with the interpretation, based on initial $^{87}Sr/^{86}Sr$ and $^{143}Nd/^{144}Nd$ data, that the coexistence of calc-alkaline and alkaline magmatism in the complex may be explained by pre-collision differences in their mantle source regions (İlbeyli *et al.* 2004; İlbeyli 2005).

### *Mechanism of Melt Genesis*

Slab detachment has been increasingly recognised in many collision-related systems (e.g., Pearce *et al.* 1990). Lithospheric thinning through delamination is induced by thermal and mechanical instability of the continental lithosphere. Rapid unroofing by isostasy is accompanied by hot asthenospheric upwelling and magmatic underplating. For the central Anatolian intrusive rocks, which are interpreted to have been derived from a subduction-modified mantle source(s), the likely mechanisms for magma generation are either lithospheric extension or uplift; or melting of mantle lithosphere by the perturbation of the geotherm due to delamination of the thermal boundary layer, or slab detachment. Perturbation of subduction-metasomatised lithosphere by either delamination of the thermal boundary layer or slab detachment may have generated the primary magmas for the central Anatolian plutonic rocks (İlbeyli *et al.* 2004). Both processes would lead to conductive heating of enriched mantle. This may have assisted or initiated the orogenic collapse that followed collision and uplift. A similar mechanism was also suggested for the origin of the east-central Anatolian intrusive rocks (Özgenç & İlbeyli 2009). This mechanism was also noted for the generation of the central Anatolian intrusive rocks (İlbeyli & Pearce 1997; Aydın *et al.* 1997; Boztuğ 1998).

## Conclusions

The intrusive rocks of the Central Anatolian Crystalline Complex can be divided into three groups on the basis of their field, petrographic, major-trace element and isotopic characteristics. These are: (i) calc-alkaline, (ii) subalkaline/transitional, and (iii) alkaline. These intrusive rocks cover a petrological range from monzodiorite through quartz monzonite to syenite/granite. Whole-rock oxygen isotope data from the complex have a range of $\delta^{18}O$ values from 6.5‰ to 14.8‰.

The oxygen isotope values show that the intrusive rocks originated from a mantle source containing large subduction components, although a within-plate component is also present in the source of alkaline rocks. All rock types have experienced crustal assimilation and fractional crystallisation. In the region, the coexistence of calc-alkaline and alkaline magmatism could be attributed to mantle source heterogeneity before collision. Delamination of the thermal boundary layer, and/or slab breakoff is the likely mechanisms for the initiation of the diverse magmatism in the complex.

## Acknowledgement

N. İlbeyli thanks SUERC-the Scottish Universities Environmental Research Centre, Stable Isotope Geosciences Laboratories at Glascow. N. İlbeyli also thanks Terry Donnelly and Chris Taylor for their help on isotope analyses. N. İlbeyli specially thanks to Donna L. Whitney. Nilgün Güleç and an anonymous reviewer are kindly thanked for their review. Erdin Bozkurt is thanked for editorial handling. John A. Winchester edited English of the final text.

## References

Aydın, N.S., Göncüoğlu, M.C. & Erler, A. 1997. Granitoid magmatism in Central Anatolia. *In*: Boztuğ, D., Yilmaz-Şahin, S., Otlu, N. & Tatar, S. (eds), *Proceedings of TÜBİTAK-BAYG/NATO-D Program on 'Alkaline Magmatism'*. (Theoretical Consideration and a Field Excursion in Central Anatolia), Department of Geological Engineering. Cumhuriyet University, Sivas, p. 202.

Bacon, C.R., Adami, L.H. & Lanphere, M.A. 1989. Direct evidence for the origin of low-d$^{18}$O silicic magmas: Quenched samples of a magma chamber's partially fused granitoid walls, Crater Lake, Oregon. *Earth and Planetary Science Letters* **96**, 199–208.

Bingöl, E. 1989. *Geological Map of Turkey, Scale 1:2,000,000*. Mineral Research and Exploration Institute of Turkey (MTA) Publications [in Turkish with English abstract].

Boynton, W.V. 1984. Geochemistry of the rare earth elements: meteorite studies. *In*: Henderson, P. (ed), *Rare Earth Element Geochemistry*. Elsevier, 63–114.

Boztuğ, D. 1998. Post-collisional central Anatolian alkaline plutonism, Turkey. *Turkish Journal of Earth Sciences* **7**, 145–165.

Boztuğ, D. & Arehart, G.B. 2007. Oxygen and sulfur isotope geochemistry revealing a significant crustal signature in the genesis of the post-collisional granitoids in central Anatolia, Turkey. *Journal of Asian Earth Sciences* **30**, 403–416.

Boztuğ, D. & Jonckheere, R.C. 2007. Apatite fission track data from central Anatolian granitoids (Turkey): constraints on Neo-Tethyan closure. *Tectonics* **26**, TC3011.

Boztuğ, D. & Harlavan, Y. 2008. K-Ar ages of granitoids unravel the stages of Neo-Tethyan convergence in the eastern Pontides and central Anatolia, Turkey. *International Journal of Earth Sciences* **97**, 585–599.

Boztuğ, D., Tichomirowa, M. & Bombach, K. 2007b. $^{207}Pb/^{206}Pb$ single-zircon evaporation ages of some granitoid rocks reveal continent-oceanic island arc collision during the Cretaceous geodynamic evolution of the Central Anatolian crust, Turkey. *Journal of Asian Earth Sciences* **31**, 71–86.

Boztuğ, D., Harlavan, Y., Arehart, G.B., Satir, M. & Avci, N. 2007a. K-Ar age, whole-rock and isotope geochemistry of A-type granitoids in the Divrigi-Sivas region, eastern-central Anatolia, Turkey. *Lithos* **97**, 193–218.

Boztuğ, D., Güney, Ö., Heizler, M., Jonckheere, R., Tichomirowa, M. & Otlu, N. 2009a. $^{207}Pb$-$^{206}Pb$, $^{40}Ar$-$^{39}Ar$ and fission-track geothermochronology quantifying cooling and exhumation history of the Kaman-Kırşehir region intrusions, Central Anatolia, Turkey. *Turkish Journal of Earth Sciences* **18**, 85–108.

Boztuğ, D., Güney, Ö., Heizler, M., Jonckheere, R. & Tichomirowa, M. 2009b. $^{207}Pb$-$^{206}Pb$, $^{40}Ar$-$^{39}Ar$ and apatit fission-track geothermochronology revealing the emplacement, cooling and exhumation history of the Karaçayır syenite (N Sivas), East-Central Anatolia, Turkey. *Turkish Journal of Earth Sciences* **18**, 109–125.

Boztuğ, D., Debon, F., İnan, S., Tutkun, Z.S., Avci, N. & Kesgin, Ö. 1997. Comparative geochemistry of four plutons from the Cretaceous–Palaeogene central eastern Anatolian alkaline province (Divrigi region, Sivas, Turkey). *Turkish Journal of Earth Sciences* **6**, 95–115.

Coplen, T.B., Kendall, C. & Hopple, J. 1983. Comparison of stable isotope reference samples. *Nature* **303**, 236–238.

Criss, R.E., Gregory, R.T. & Taylor, H.P. 1987. Kinetic theory of oxygen isotope exchange between minerals and water. *Geochimica et Cosmochimica Acta* **51**, 952–960.

Davidson, J.P. 1996. Deciphering mantle and crustal signature in subduction zone magmatism. *In*: Bebout, G.E., Scholl, D.W., Kirby, S.H. & Platt, J.P. (eds), *Subduction Top to Bottom*. Geophysical Monograph **96**, 251–262.

Davidson, J.P., McMillan, N.J., Moorbath, S., Worner, G., Harmon, R.S. & Lopez-Escobar, L. 1990. The Nevados de Pavachata volcanic region, 18°S/69°W, N Chile, II. Evidence for widespread crustal involvement in Andean magmatism. *Contributions to Mineralogy and Petrology* **105**, 412-443.

DePaolo, D.J. 1981. Trace element and isotopic effects of combined wallrock assimilation and fractional crystallization. *Earth and Planetary Science Letters* **53**, 189–202.

DePaolo, D.J. 1988. *Neodymium Isotope Geochemistry. An Introduction.* Minerals and Rocks 20, Springer-Verlag, New York.

Eiler, J.M., Schiano, P., Kitchen, N. & Stolper, E. 2000. Oxygen isotope evidence for recycled crust in the sources of mid-ocean ridge basalts. *Nature* **403**, 530–534.

Ellam, R.M. & Harmon, R.S. 1990. Oxygen isotope constraints on the crustal contribution to the subduction-related magmatism of the Aeolian Islands, southern Italy. *Journal of Volcanology and Geothermal Research* **44**, 105–122.

Feeley, T. & Sharp, Z.D. 1995. $^{18}O/^{16}O$ isotope geochemistry of silicic lava flows erupted from Volcán Ollagüe, Andean Central Volcanic Zone. *Earth and Planetary Science Letters* **133**, 239–254.

Gill, J.B. 1981. *Orogenic Andesites and Plate Tectonics*. Springer-Verlag, Berlin.

Giret, A. & Lameyre, J. 1980. Mise en place et evolution magmatique des complexes plutoniques de la caldera de Courbet, ile Kerguelen. *Bulletin of Geological Society (France)* **7-XXII-3**, 437–446.

Göncüoğlu, M.C., Toprak, V., Kuşçu, İ., Erler, A. & Olgun, E. 1991. *Geology of the Western Part of the Central Anatolian Massif. Part I: Southern Section.* Turkish Petroleum Corporation (TPAO) Report no. **2909** [in Turkish, unpublished].

Gregory, R.T. & Criss, R.E. 1986. Isotopic exchange in open and closed systems. *In*: Valley, J.W., Taylor, H.P. & O'Neil, J.R. (eds), *Stable Isotopes in High Temperature Geological Processes*. Reviews in Mineralogy **16**, 91–127.

Halama, R., Marks, M., Brügmann, G., Siebel, W., Wenzel, T. & Markl, G. 2004. Crustal contamination of mafic magmas: evidence from a petrological, geochemical and Sr-Nd-Os-O isotopic study of the Proterozoic Isortoq dike swarm, South Greenland. *Lithos* **74**, 199–232.

Harris, C., Faure, K., Diamond, R.E. & Scheepers, R. 1997. Oxygen and hydrogen isotope geochemistry of S- and I-type granitoids: the Cape Granite suite, South Africa. *Chemical Geology* **143**, 95–114.

Hildreth, W. & Moorbath, S. 1988. Crustal contribution to arc magmatism in the Andes of southern Chile. *Contributions to Mineralogy and Petrology* **98**, 455–489.

İlbeyli, N. 1999. *Petrogenesis of Collision-related Plutonic Rocks, Central Anatolia (Turkey).* PhD Thesis, University of Durham, Durham, UK [unpublished].

İlbeyli, N. 2004. Field, petrographic and geochemical characteristics of the Hamit alkaline intrusion in the Central Anatolian Crystalline Complex, Turkey. *Turkish Journal of Earth Sciences* **13**, 269–286.

İlbeyli, N. 2005. Mineralogical-geochemical constraints on intrusives in central Anatolia (Turkey): tectono-magmatic evolution and characteristics of mantle source. *Geological Magazine* **142**, 187–207.

İlbeyli, N. & Pearce, J.A. 1997. Petrogenesis of the collision-related central anatolian granitoids, Turkey. European Union of Geosciences Meeting (EUG9), Strasbourg, France. *Terra Abstracts* **9**, p. 502.

İlbeyli, N., Pearce, J.A., Thirlwall, M.F. & Mitchell, J.G. 2004. Petrogenesis of collision-related plutonics in central Anatolia, Turkey. *Lithos* **72**, 163–182.

James, D.E. 1981. The combined use of oxygen and radiogenic isotopes as indicators of crustal contamination. *Annual Review of Earth and Planetary Sciences* **9**, 311–320.

Jung, S., Mezger, K. & Hoernes, S. 2004. Shear zone-related syenites in the Damara belt (Namibia): the role of crustal contamination and source composition. *Contributions to Mineralogy and Petrology* **148**, 104–121.

Jung, S., Mezger, K., Hoernes, S. & Hoffbauer, R. 2007. Altered mafic lower continental crust as a source for low $\delta^{18}$O-granodiorites (Damara orogen, Namibia)? *Mineralogy and Petrology* **91**, 1–10.

King, E.M., Valley, J.W., Davis, D.W. & Edwards, G.R. 1998. Oxygen isotope ratios of Archean plutonic zircons from granite-greenstone belts of the Superior Province: indicator of magmatic source. *Precambrian Research* **92**, 365–387.

Köksal, S., Romer, R.L., Göncüoğlu, M.C. & Toksoy-Köksal, F. 2004. Timing of post-collisional H-type to A-type granitic magmatism: U-Pb titanite ages from Alpine central Anatolian granitoids (Turkey). *International Journal of Earth Sciences* **93**, 974–989.

Larson, P.B. & Taylor, H.P. 1986. $^{18}O/^{16}O$ ratios in ash-flow tuffs and lavas erupted from the central Nevada caldera complex and the central San Juan caldera complex, Colorado. *Contributions to Mineralogy and Petrology* **92**, 146–156.

Macpherson, C.G., Gamble, J.A. & Mattey, D.P. 1998. Oxygen isotope geochemistry of lavas from an oceanic to continental arc transition, Kermadec-Hikurangi margin, SW Pacific. *Earth and Planetary Science Letters* **160**, 609–621.

Mason, P., Downes, H., Thirlwall, M.F., Seghedi, I., Szakács, A., Lowry, D. & Mattey, D. 1996. Crustal assimilation as a major petrogenetic process in the east Carpathian Neogene and Quaternary continental margin arc, Romania. *Journal of Petrology* **37**, 927–959.

Middlemost, E.A.K. 1994. Naming materials in the magma/igneous rock system. *Earth-Science Reviews* **37**, 215–224.

Miyashiro, A. 1978. Nature of alkalic volcanic rock series. *Contributions to Mineralogy and Petrology* **66**, 91–104.

Monani, S. & Valley, J.W. 2001. Oxygen isotope ratio of zircon: magma genesis of low d$^{18}$O granites from the British Tertiary Igneous Province, western Scotland. *Earth and Planetary Science Letters* **184**, 377–392.

Önal, A., Boztuğ, D., Kürüm, S., Harlavan, Y., Arehart, G.B. & Arslan, M. 2005. K-Ar age determination, whole-rock oxygen isotope geochemistry of the post-collisional Bizmisen and Calti plutons SW Erzincan, eastern Central Anatolia, Turkey. *Geological Journal* **40**, 457–476.

Özgenç, İ. & İlbeyli, N. 2009. Geochemical constraints on petrogenesis of Late Cretaceous alkaline magmatism in east-central Anatolia (Hasançelebi-Başören, Malatya), Turkey. *Mineralogy and Petrology* **95**, 71–85.

Pearce, J.A., Harris, N.B.W. & Tindle, A.G. 1984. Trace element discrimination diagrams for the tectonic interpretation of granitic rocks. *Journal of Petrology* **25**, 956–983.

Pearce, J.A., Bender, J.F., De Long, S.E., Kidd, W.S.F., Low, P.J., Güner, Y., Şaroğlu, F., Yilmaz, Y., Moorbath, S. & Mitchell, J.G. 1990. Genesis of collision volcanism in eastern Anatolia, Turkey. *Journal of Volcanology and Geothermal Research* **44**, 189–229.

Platt, J.P. & England, P.C. 1993. Convective removal of lithosphere beneath mountain belts: thermal and mechanical consequences. *American Journal of Science* **293**, 307–336.

Seghedi, I., Downes, H., Szakacs, A., Mason, P.R.D., Thirlwall, M.F., Rosu, E., Pecskay, Z., Marton, E. & Panaiotu, C. 2004. Neogene–Quaternary magmatism and geodynamics in the Carpathian-Pannonian region: a synthesis. *Lithos* **72**, 117–146.

Sharp, Z.D. 1990. A laser-based microanalytical method for the in situ determination of oxygen isotope ratios of silicates and oxides. *Geochimica et Cosmochimica Acta* **54**, 1353–1357.

Sheppard, S.M.F. & Harris, C. 1985. Hydrogen and oxygen isotope geochemistry of Ascension Island lavas and granites: variation with crystal fractionation and interaction with sea water. *Contributions to Mineralogy and Petrology* **91**, 74–81.

Singer, B.S., Leeman, W.P, Thirlwall, M.F. & Roger, N.W.E. 1996. Does fracture zone subduction increase sediment flux and mantle melting in subduction zones? Trace element evidence from Aleutian arc basalt. *In*: Bebout, G.E., Scholl, D.W., Kirby, S.H. & Platt, J.P. (eds), *Subduction Top to Bottom*. Geophysical Monograph **96**, 285–291.

Sun, S. & McDonough, W.F. 1989. Chemical and isotopic systematics of oceanic basalts: implications for mantle compositions and processes. *In*: Saunders, A.D. & Norry, M.J. (eds), *Magmatism in the Ocean Basins*. Geological Society, London, Special Publications **42**, 313–345.

Şengör, A.M.C. & Yilmaz, Y. 1981. Tethyan evolution of Turkey: a plate tectonic approach. *Tectonophysics* **75,** 181–241.

Tatar, S. & Boztuğ, D. 2005. The syn-collisional Danacıobaşı biotite leucogranite derived from the crustal thickening in central Anatolia (Kırıkkale), Turkey. *Geological Journal* **40**, 571–591.

Taylor, H.P.Jr. 1986. Igneous rocks: II. Isotopic case studies of circumpacific magmatism. *Reviews in Mineralogy and Geochemistry* **16**, 273–316.

Taylor, H.P.Jr. 1997. Oxygen and hydrogen isotope relationships in hydrothermal mineral deposits. *In*: Barnes, H.L. (ed), *Geochemistry of Hydrothermal Ore Deposits*. John Wiley and Sons, New York, 229–302.

Thirlwall, M.F., Smith, T.E., Graham, A.M., Theodorou, N., Hollings, J.P., Davidson, J.P. & Arculus, R.J. 1994. High field strength element anomalies in arc lavas: source or process? *Journal of Petrology* **35**, 819–838.

Turner, S., Arnaud, N., Liu, J., Rogers, N., Hawkesworth, C., Harris, N., Kelley, S., Van Calsteren, P. & Deng, W. 1996. Post-collision, shoshonitic volcanism on the Tibetan plateau: implications for convective thinning of the lithosphere and the source of ocean island basalts. *Journal of Petrology* **27**, 45–71.

Valley, J.W., Chiarenzelli, J.R. & McLelland, J.M. 1994. Oxygen isotope geochemistry of zircon. *Earth and Planetary Science Letters* **126**, 187–206.

Valley, J.W., Lackey, J.S., Cavosie, A.J., Clechenko, C.C., Spicuzza, M.J., Basei, M.A.S., Bindeman, I.N., Ferreira, V.P., Sial, A.N., King, E.M., Peck, W.H., Sinha, A.K. & Wei, C.S. 2005. 4.4 billion years of crustal maturation: oxygen isotope ratios of magmatic zircon. *Contributions to Mineralogy and Petrology* **150**, 561–580.

Whalen, J.B., Jenner, G.A., Longstaffe, F.J., Robert, F. & Gariepy, C. 1996. Geochemical and isotopic (O, Nd, Pb and Sr) constraints on A-type granite petrogenesis based on the Topsails igneous suite, Newfoundland Appalachians. *Journal of Petrology* **376**, 7–60.

Whitney, D.L. & Hamilton, M.A. 2004. Timing of high-grade metamorphism in central Turkey and the assembly of Anatolia. *Journal of the Geological Society, London* **161**, 823–828.

Whitney, D.L., Teyssier, C., Dilek, Y. & Fayon, A.K. 2001. Metamorphism of the Central Anatolian Crystalline Complex, Turkey: influence of orogen-normal collision vs. wrench dominated tectonics on P-T-t paths. *Journal of Metamorphic Geology* **19**, 411–432.

Whitney, D.L., Teyssier, C., Fayon, A.K., Hamilton, M.A. & Heizler, M. 2003. Tectonic controls on metamorphism, partial melting, and intrusion: timing and duration of regional metamorphism and magmatism in the Niğde Massif, Turkey. *Tectonophysics* **376**, 37–60.

Yaliniz, K. & Göncüoğlu, M.C. 1998. General geological characterictics and distribution of central Anatolian ophiolites. *Geosound* **20**, 19–30 [in Turkish].

Yaliniz, K., Floyd, P.A. & Göncüoğlu, M.C. 1996. Supra-subduction zone ophiolite in central Anatolia: Geochemical evidence from the basalts of the Sarıkaraman Ophiolite (Aksaray-Turkey). *Mineralogical Magazine* **60**, 697–710.